

**Effects of molecular resonances on Rydberg blockade**Andrei Derevianko,<sup>1,2</sup> Péter Kómár,<sup>3</sup> Turker Topcu,<sup>1,2</sup> Ronen M. Kroeze,<sup>3,4</sup> and Mikhail D. Lukin<sup>3</sup><sup>1</sup>*Department of Physics, University of Nevada, Reno, Nevada 89557, USA*<sup>2</sup>*ITAMP, Harvard-Smithsonian Center for Astrophysics, Cambridge, Massachusetts 02138, USA*<sup>3</sup>*Department of Physics, Harvard University, Cambridge, Massachusetts 02138, USA*<sup>4</sup>*Department of Physics, Eindhoven University of Technology, 5600 MB Eindhoven, the Netherlands*

(Received 27 July 2015; published 23 December 2015)

We study the effect of resonances associated with complex molecular interaction of Rydberg atoms on Rydberg blockade. We show that densely spaced molecular potentials between doubly excited atomic pairs become unavoidably resonant with the optical excitation at short interatomic separations. Such molecular resonances limit the coherent control of individual excitations in Rydberg blockade. As an illustration, we compute the molecular interaction potentials of Rb atoms near the 100s states asymptote to characterize such detrimental molecular resonances and determine the resonant loss rate to molecules and inhomogeneous light shifts. Techniques to avoid the undesired effect of molecular resonances are discussed.

DOI: [10.1103/PhysRevA.92.063419](https://doi.org/10.1103/PhysRevA.92.063419)

PACS number(s): 32.80.Ee, 42.50.Dv, 03.67.—a, 32.80.Rm

**I. INTRODUCTION**

Rydberg blockade [1–4] has recently emerged as a promising method for creating and manipulating quantum states of light and matter in applications ranging from quantum information processing [5–7] to quantum nonlinear optics [8,9]. The key idea is that strong interaction between Rydberg atoms can be used, under certain conditions, to block the states with more than one excited atoms. Multiple Rydberg excitations are suppressed due to level shifts caused by strong long-range interactions between Rydberg atoms. This mechanism enables performing quantum logic operations between atom pairs and manipulate collective many-body states of an  $N$ -atom ensemble [1]. Such collective states efficiently couple to laser fields with the coupling enhanced by a factor of  $\sqrt{N}$ ; see experiments [10,11]. While a number of advanced protocols involving Rydberg blockade are being explored, an outstanding challenge is to identify and realize conditions for high-fidelity atomic and optical state control via Rydberg blockade.

Here we investigate the effect of molecular resonance on quantum state manipulation via Rydberg blockade. We demonstrate that the very same interactions that cause the level shifts required for blockade also have detrimental effects due to a large state density (number of levels per energy interval) of Rydberg states resulting in a plethora of closely spaced molecular potentials. Some of these potentials may become, at specific interatomic separation, resonant with the driving field causing excitations to unwanted doubly excited Rydberg states. While this mechanism was qualitatively pointed out [12,13], detailed understanding of effects of molecular resonances on collective state manipulation is important for high fidelity quantum states control. This is challenging partially due to the overwhelming complexity of molecular potentials especially at small internuclear separations [12]. Below we demonstrate that the cumulative effect on the Rydberg blockade is caused by molecular resonances at large interatomic distances where reliable theoretical predictions can be made. We derive and compute the rates of resonant conversions to diatoms, show that collective qubit rotations are damped, and compute the “leakage” and inhomogeneous frequency shifts

due to diatom conversion. Finally, we discuss techniques to suppress the deleterious molecular resonance effects.

**II. MOLECULAR RESONANCES**

We start by computing molecular potentials for two interacting Rb Rydberg atoms by a direct diagonalization of the long-range dipole-dipole molecular Hamiltonian. On a large energy scale, we find a “spaghetti” of densely packed curves exhibiting intricate avoided crossing patterns. The region that is relevant to our discussion is centered around the nominally blocked Rydberg levels. As an illustration, we take  $|r\rangle = |100s\rangle$ . Considering that the typical excitation Rabi frequency  $\Omega_0$  is  $\sim 1$  MHz we zoom onto a 1 GHz window (Fig. 1) centered about the  $100s + 100s$  dissociation limit. In this figure the potential that at large  $R$  asymptotes to two  $100s$  atoms is the blockading van der Waals interaction. However, we also find several potential curves that at short  $R$  cross zero energy corresponding to a resonance with the laser field. As a result, atoms can be promoted into an undesired molecular state corresponding to two Rydberg atoms. Properties of these resonant crossings are compiled in Table I. The outermost crossing with the most substantial laser coupling is at  $R_x \approx 6.2 \mu\text{m}$ . Since this value is larger than the average interatomic separation for typical experimental number densities [10]  $\rho_d \approx 10^{11} - 10^{12} \text{ cm}^{-3}$ , one may find a fraction of atomic pairs inside the volume-enclosing molecular resonance region.

Note that the potential curves were computed in the basis of atomic orbitals with orbital angular momenta up to  $\ell_{\text{max}} = 2$ . Increasing  $\ell_{\text{max}}$  and adding atomic orbitals to the computational basis breed new resonant crossings, as the system becomes increasingly chaotic at smaller  $R$  due to stronger interchannel couplings and thus larger number of avoided crossings. Even our outermost resonance can be superseded by crossings at larger  $R$ , but with suppressed laser couplings. However, the parameters of the outermost crossing in Fig. 1 are stable with respect to the basis variation. As we demonstrate below this outermost crossing predominantly affects the dynamics of collective excitations thereby mitigating challenges of reliably computing full-scale Ry-Ry interaction potentials.

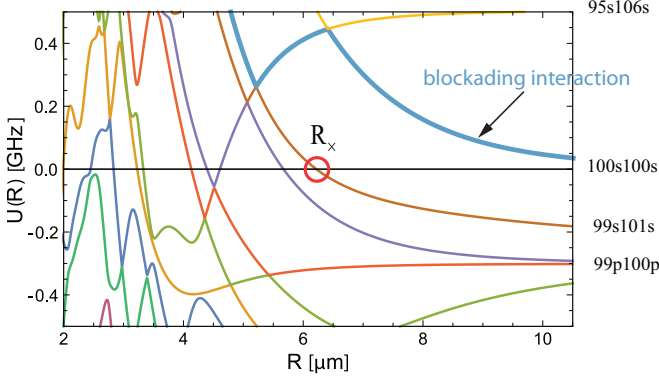


FIG. 1. (Color online) Selected  $\Sigma_g$  molecular potentials in the 1 GHz window centered about the  $100s + 100s$  dissociation limit (placed at zero energy) for two Rb atoms. The potentials are marked by their double-atom dissociation limits at large internuclear separations  $R$ . Highlighted blockading interaction is the interaction that tunes a pair of  $100s$  Ry atoms away from the resonance with driving laser field. The position  $R_x$  of the outermost resonant molecular potential crossing is marked with a circle. Properties of molecular resonances are compiled in Table I.

Despite the complexity of molecular potentials, the position  $R_x$  of the outermost resonance can be estimated as follows. Suppose the  $ns + ns$  state is our  $|rr\rangle$  “blockaded” state. The nearest-energy  $n's + n''s$  state with  $n' \approx n'' \approx n$  is the  $(n-1)s + (n+1)s$  state, and at large  $R$  it lies below the resonance by  $\delta_m \approx -3n^{-4}$ . Further, the molecular potential correlating to the  $(n-1)s + (n+1)s$  atoms behaves as  $n^4 \tilde{c}_3 / R^3$  due to the repulsion from the  $p + p$  state below, where  $\tilde{c}_3 \sim 1$ . Thereby,  $U(R) \approx -3n^{-4} + n^4 \tilde{c}_3 / R^3$ , and from  $U(R_x) = 0$  we arrive at  $R_x \approx (3^{-1} \tilde{c}_3 n^8)^{1/3}$ . For  $n = 100$  this estimate with  $\tilde{c}_3 = 1$  leads to  $R_x \approx 8 \mu\text{m}$  in a reasonable agreement with our computed value. Further, we evaluated molecular Rabi frequencies  $\Omega_m = \xi_m \Omega_0$  (typically a fraction  $\xi_m$  of  $\Omega_0$ ; see Table I). For the outermost resonance, such couplings originate from admixtures of the  $100s + ns$  states through the

TABLE I. Molecular resonance shell properties for the Rb  $100s$  blockaded state (see Fig. 1).  $R_x$  and  $\Delta R_x$  are the shell radii and widths,  $\xi_m$  are the fractional molecular Rabi frequencies,  $\xi_m = \Omega_m / \Omega_0$ , and  $\gamma_m$  are molecular loss rates.  $\Delta R_x$  and  $\gamma_m$  are evaluated for atomic Rabi frequency  $\Omega_0 = (2\pi) \times 0.1$  MHz and number density  $\rho_d = 10^{12} \text{ cm}^{-3}$ . Positions and the number of resonances for smaller  $R$  are computational-basis dependent; however, their contribution to the total rate is strongly suppressed.

$R_x, \mu\text{m}$	$\xi_m$	$\Delta R_x, \mu\text{m}$	$\gamma_m, \text{s}^{-1}$
6.22	0.55	$3.8 \times 10^{-4}$	$1.0 \times 10^5$
5.67	0.091	$3.5 \times 10^{-5}$	$1.3 \times 10^3$
4.61	0.012	$2. \times 10^{-6}$	$6.2 \times 10^0$
4.39	0.44	$8.6 \times 10^{-5}$	$9.1 \times 10^3$
4.13	0.13	$1.7 \times 10^{-5}$	$4.6 \times 10^2$
3.33	0.16	$9.3 \times 10^{-6}$	$2.0 \times 10^2$
2.45	0.011	$1.2 \times 10^{-6}$	$9.8 \times 10^{-1}$
1.99	0.0017	$6.4 \times 10^{-8}$	$5.4 \times 10^{-3}$
...			

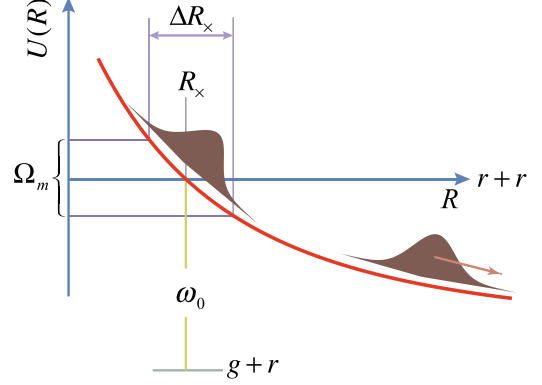


FIG. 2. (Color online) A laser pulse nominally resonant with the  $r - g$  transition can resonantly excite molecular states. The molecular wave packet is efficiently excited within a window  $\Delta R_x$  determined by the slope of molecular potential  $U(R)$  and molecular Rabi frequency  $\Omega_m$ . Once excited the wave packet rapidly accelerates out of resonance and rolls down the slope of molecular potential.

off-diagonal van der Waals interaction. We evaluated  $\xi_m$  from the eigenvectors of the numerically diagonalized molecular Hamiltonian.

The atoms are efficiently laser-coupled to the molecular resonances only in a small window of  $R$ , when the detuning  $U(R)$  is comparable to  $\Omega_m$  (see Fig. 2). Thereby we define an effective radial width of the molecular resonance

$$\Delta R_x = \Omega_m(R_x) / |U'(R_x)|, \quad (1)$$

where  $\Omega_m$  and the derivative of the molecular potential  $U'(R_x) = dU(R_x)/dR$  are evaluated at the resonance crossing. For the outermost resonance  $\Delta R_x \approx \Omega_0 \xi_m n^{20/3} (\tilde{c}_3/3)^{1/3} / 9$ . Each molecular resonance therefore defines a “resonance shell,” a spherical shell of radius  $R_x$  and radial width  $\Delta R_x$  centered at a given atom. The average number of atoms inside the resonance shell,

$$\Delta N_x = 4\pi R_x^2 \Delta R_x \rho_d, \quad (2)$$

is a relatively small number in a typical experiment. For parameters of Table I, the outermost resonance shell contains fewer than  $\sim 0.1$  atoms.

### III. ATOM LOSS

The presence of molecular resonances implies several consequences for the Rydberg blockade, the most important being the atomic loss. Indeed, inside the shell two excited Rydberg atoms are subject to a mechanical force  $-U'(R_x)$ . This force can be either attractive or repulsive. (An example of the repulsive resonance is at  $R_x \approx 6.2 \mu\text{m}$ ; see Fig. 2.) The diatom would separate into two  $99s$  and  $101s$  Ry atoms with a kinetic energy of relative motion equal to the dissociation limit  $\delta_m \approx -3n^{-4}$ , which is  $\sim 10$  mK for  $n = 100$ . These atoms may escape the trapping volume, effectively reducing the number of blockaded atoms. Since the atoms are accelerated out of the resonance shell on time scales  $\tau_a = \sqrt{\Delta R_x} M_a / |U'(R_x)| \ll 1/\Omega_0$ , we adopt a simple model that once a pair of atoms is promoted to a molecule, the associated motional wave packet

quickly leaves the resonance shell with its atomic constituents no longer interacting with the laser field.

The attractive potentials (see crossing at  $R_\times \approx 4.6 \mu\text{m}$  in Fig. 1) can lead to auto-ionization in the small  $R$  region [14]. Such a process would free an electron and a molecular ion, with their Coulomb fields blocking the entire sample. While in our illustrative example laser coupling to attractive potentials is negligible, it may not be the case in general. Qualitatively, to reduce autoionization one needs to pick Rydberg states such that the potentials inside the most strongly coupled resonance shells are repulsive.

### A. Dynamics of collective excitation

Now we analyze the dynamics of collective atomic ensemble excitations. We will derive the expressions for the damping (loss) rate in two approximations: (i) assuming that atoms are frozen in space (static limit) and (ii) collisional model (impact limit). Remarkably both approximations yield identical loss rate. We consider an ensemble of  $N$  atoms initially in the collective ground state  $|G\rangle = |g_1 g_2 \cdots g_N\rangle$ . A laser pulse couples  $|G\rangle$  to a superposition of singly excited Rydberg atoms  $|R_i\rangle = |g_1 \cdots g_{i-1} r_i g_{i+1} \cdots g_N\rangle$ . These atoms can be further promoted to doubly Ry-excited diatom states  $|M_{ij}\rangle$ , involving atoms  $i$  and  $j$ . There are  $N_m = N(N-1)/2$  diatom states, with their resonance detunings  $\Delta(R_{ij}) = U(R_{ij})$  and Rabi frequencies  $\Omega_m^{ij}(R_{ij})$  determined by their interatomic separations  $R_{ij}$ . Expanding the total wave function in this basis ( $\omega_0$  is the laser frequency resonant with the  $g$ - $r$  transition),

$$|\Psi\rangle = c_g e^{i\omega_0 t} |G\rangle + \sum_i c_i |R_i\rangle + e^{-i\omega_0 t} \sum_i \sum_{j>i} m_{ij} |M_{ij}\rangle,$$

and applying the rotating-wave approximation, we arrive at

$$\begin{aligned} i\dot{c}_g &= \frac{1}{2}\Omega_0 \sum_i c_i, \\ i\dot{c}_i &= \frac{1}{2}\Omega_0 c_g + \frac{1}{2} \left( \sum_{j=1}^{i-1} \Omega_m^{ij} m_{ji} + \sum_{j=i+1}^N \Omega_m^{ij} m_{ij} \right), \\ i\dot{m}_{ij} &= \Delta_{ij} m_{ij} + \frac{1}{2} \Omega_m^{ij} (c_i + c_j). \end{aligned}$$

When all molecular detunings  $\Delta_{ij}$  are large, the system undergoes the ideal Rabi flopping between the collective ground state and symmetric combination of single Rydberg excitations [ $c_g^I(t) = \cos(\sqrt{N}\Omega_0 t/2)$  and  $c_i^I(t) = -i \sin(\sqrt{N}\Omega_0 t/2)/\sqrt{N}$ ]. We focus on the averaged collective dynamics and introduce the collective amplitude  $c_s$  so that  $c_i(t) \equiv c_s(t)/\sqrt{N}$ . We assume that all  $\Omega_m^{ij} = \Omega_m$  owing to the weak  $R_{ij}$  dependence inside the resonance shell. The collective amplitudes satisfy ( $\Omega_0^N = \sqrt{N}\Omega_0$ )

$$\begin{aligned} i\dot{c}_g &= \frac{\Omega_0^N}{2} c_s, \\ i\dot{c}_s &= \frac{\Omega_0^N}{2} c_g + \frac{\Omega_m}{2\sqrt{N}} \sum_i \left( \sum_{j=1}^{i-1} m_{ji} + \sum_{j=i+1}^N m_{ij} \right), \\ i\dot{m}_{ij} &= \Delta_{ij}(R_{ij}) m_{ij} + (\Omega_m/\sqrt{N}) c_s. \end{aligned} \quad (3)$$

### B. Loss rate

Now we fix the positions of all atoms (this requirement is relaxed later) and split the time axis into time intervals consisting of a short laser pulse of duration  $\tau_p \ll 1/\Omega_0^N$  and field-free acceleration time  $\tau_a$  during which the excited diatom wave packet leaves the shell. Because of the mechanical forces the molecular amplitudes inside the shell are reset to zero values before the next pulse arrives (this is reminiscent of the Markov approximation [15]). By taking the limit  $\tau_a \rightarrow 0$  we arrive at a continuous Rabi drive. Integrating the last equation over time interval  $(t, t + \tau_p)$ , one obtains,  $m_{ij}(t + \tau_p) = c_s(t)(\Omega_m/\sqrt{N})\{\exp(i\Delta_{ij}\tau_p) - 1\}/\Delta_{ij}$ . We have set  $m_{ij}(t) = 0$  as discussed. Notice that the r.h.s. spikes at  $\Delta_{ij} = 0$ , i.e., within the resonance shell. Ensemble averaging yields  $\langle m_{ij}(t + \delta t) \rangle = -i c_s(t) \pi (\Omega_m/\sqrt{N}) (4\pi R_\times^2) / [U'(R_\times) |V_s|]$ , where  $V_s$  is the blockaded ensemble volume. By substituting this relation into the equation for  $c_s$  we arrive at a set of damped equations (non-Hermitian Schrodinger equation):

$$\begin{aligned} i\dot{c}_g &= \frac{\Omega_0^N}{2} c_s, \\ i\dot{c}_s &= \frac{\Omega_0^N}{2} c_g - i\gamma_m c_s \end{aligned} \quad (4)$$

with the molecular-resonance (amplitude) loss rate

$$\gamma_m = \pi \Delta N_\times \Omega_m / 2 = 2\pi^2 \rho_d \xi_m^2 R_\times^2 \Omega_0^2 / |U'(R_\times)|. \quad (5)$$

For the outermost resonance,  $\gamma_m \approx 2\pi^2 \rho_d \xi_m^2 \Omega_0^2 \tilde{c}_3 n^{12} / 27$ . The above derivation neglected atomic motion and is valid for very cold ensembles. In Appendix A, we take into account the thermal motion of the atoms, using the impact approximation. We find the result for  $\gamma_m$  that is identical to Eq. (5).

The rate formula is to be summed over all resonance shells:  $\gamma_m^{\text{tot}} = \sum_k \gamma_m^k$ , where  $\gamma_m^k$  is the individual shell contribution (5). For our example in Table I,  $\gamma_m^{\text{tot}}$  is entirely dominated by the outermost crossing. The reason for this prominence is that at smaller  $R$ , the potentials become steeper and the molecular Rabi frequencies become diluted, thereby leading to smaller values of  $\Delta R_\times$  [see Eq. (1) and Table I] and together with smaller values of  $R_\times$  leading to smaller values of  $\Delta N_\times$  and thereby  $\gamma_m$ . Notice that the long-range molecular Hamiltonian used in computing the molecular potential curves in Fig. 1 holds only for  $R \gg 2n^2 a_0 \sim 1 \mu\text{m}$  for  $n = 100$ , i.e., when the electronic densities do not overlap. However, all the qualitative arguments that the molecular excitation rates should be suppressed compared to the outermost resonance shell still hold even for small  $R$ .

The rate scales steeply with  $n$ ,  $\gamma_m \propto n^{12}$ . In particular, it is commonly believed that the blockade fidelity can be improved by going to high- $n$  Ry states, because the probability of off-resonant Ry excitations is suppressed as  $n^{-22}$  in the van der Waals blockade. We see that increasing  $n$  while suppressing off-resonant Ry excitations also increases the undesired molecular loss rates.

In addition to the loss, the same  $\Omega$  drive induces an AC Stark shift which is different for states in which different atoms are excited. This inhomogeneous broadening results in an additional loss of coherence of the Rabi oscillation. In

Appendix B, we show that this broadening is given by

$$\delta\Delta \approx (7\pi/2)\rho_d\xi_m^2 R_\times^2 \Omega_0^2 / |U'(R_\times)| \quad (6)$$

in the limit where  $R_\times$  is much smaller than the size of the ensemble. Although the dependence of the system parameters is the same as for  $\gamma_m$  in Eq. (5), the prefactor makes  $\delta\Delta$  roughly two times smaller than  $\gamma_m$ . During the Rabi dynamics, the broadening makes the signal decay as  $\exp[-(\delta\Delta t)^2]$  over time, and hence the molecular loss is dominant as long as  $\gamma_m t < 1$ .

### C. Damped Rabi oscillations

Equations (4) reduce to the damped oscillator equation of motion  $\ddot{c}_s + (\Omega_0^N/2)^2 c_s - \gamma_m c_s = 0$  with solutions

$$c_s(t) = -i(\Omega_0^N/\Omega_d) \sin(\Omega_d t/2) e^{-\frac{\gamma_m}{2}t}, \quad (7)$$

$$c_g(t) = [\cos(\Omega_d t/2) + (\gamma_m/\Omega_d) \sin(\Omega_d t/2)] e^{-\frac{\gamma_m}{2}t}, \quad (8)$$

where  $\Omega_d = \Omega_0^N(1 - \eta^2)^{1/2}$ ,  $\eta = \gamma_m/\Omega_0^N$ . The driven ensemble exhibits damped collective Rabi oscillations with a frequency  $\Omega_d \leq \Omega_0^N$ . One may distinguish between three classes of solutions [16]: underdamped ( $\eta < 1$ ), critical ( $\eta = 0$ ), and overdamped ( $\eta > 1$ ). Explicitly,

$$\eta = 2\pi^2 \frac{\sqrt{N}}{V_s |U'(R_\times)|} \xi_m^2 R_\times^2 \Omega_0 \propto n^{12} \sqrt{N} \Omega_0.$$

Thereby increasing  $\Omega_0, n$ , or  $\rho_d$  can cause the ensemble to exhibit overdamping of collective Rabi oscillations, at which point they no longer resemble oscillations. In the underdamped regime, the loss per collective Rabi cycle determines collective qubit operation fidelity  $F = (\Omega_0^N/\Omega_d)^2 e^{-2\pi\eta}$ .

The molecular loss can account for some experimentally observed imperfections. For example, Dudin *et al.* [10] have effectively measured the damping constant for collective Rabi oscillations in a mesoscopic ensemble of 102s Rb atoms. They found that the Rabi oscillation loses 10%–20% of its contrast in a single cycle. Our calculation can account for a loss of ~5% during a single oscillation cycle. While the agreement seems to be adequate, we emphasize that it may be fortuitous as the experiment has been carried out in the presence of magnetic field which was excluded in our analysis and would introduce additional resonances. We also neglected the  $s$ - $d$  excitation channels (allowed in the excitation scheme [10]) when computing molecular Rabi frequencies. Moreover, the experiment [10] (and similar experiments [5,11,17,18]) are affected by a multitude of other decoherence effects. At this point it may be desirable to design experiments that could disentangle various decoherence mechanisms, and the molecular losses in particular.

### D. Effective atom number

While the total number of atoms  $N$  remains constant during the coherent evolution, the wave function acquires outcoupled diatom wave packets. If the measurement of the total number of atoms were to be made, the number of atoms remaining in the ensemble would be  $N_{\text{eff}}(t) = N(|c_g(t)|^2 + |c_s(t)|^2)$ . By manipulating Eq. (4), one finds that  $\dot{N}_{\text{eff}} = -2\gamma_m |c_s(t)|^2 N$ , resulting in  $N_{\text{eff}}(t) =$

$N\{1 + 2(\frac{\gamma_m}{\Omega_d})^2 \sin^2(\frac{\Omega_d t}{2}) + (\frac{\gamma_m}{\Omega_d}) \sin(\Omega_d t)\} e^{-\gamma_m t}$ , or averaging over many cycles  $\bar{N}_{\text{eff}}(t) = N[1 + (\gamma_m/\Omega_d)^2] e^{-\gamma_m t}$ , i.e., the effective number of atoms remaining in the ensemble decays exponentially. The quantity  $1 - (|c_g|^2 + |c_s|^2) = [N - N_{\text{eff}}(t)]/N \sim (\gamma_m/\Omega_d)^2 e^{-\gamma_m t}$  also determines “leakage” from the collective qubit space. Clearly, to minimize the leakage one has to require that  $\gamma_m t \ll 1$  or  $\gamma_m \ll \Omega_0 \sqrt{N}$ . For parameters of Table I, the coherent evolution is limited to  $t \ll 10 \mu\text{s}$ .

One may visualize the “leakage” from the collective qubit space as a modulated outflow of molecular wave packets from the blockaded volume. As an illustration, the outermost molecular resonance produces admixtures of 101s and 99s Rydberg atoms. If the ensemble is trapped, the outcoupled (di)atoms may linger inside the ensemble depending on the released kinetic energy and the trapping potential height. Such atoms do not resonantly interact with the laser field of the Rabi drive. However, they do interact with the remaining ensemble leading to energy shifts through the interactions with the remaining atoms. Such mechanisms can be also relevant for untrapped ensembles, where the outflowing diatom wave packets may interact with the remaining ensemble while transiting out through the volume. In addition, the present discussion focused on Rydberg  $S$  states, the undesired effects can be enhanced for Rydberg states with higher angular momentum. This is due to the presence of closely spaced states, due to, e.g., spin-orbit interaction, that can result in molecular crossing at larger  $R$ .

## IV. SUPPRESSION WITH LATTICE

The unwanted effect of molecular resonances can be suppressed by using tight traps for individual atoms prior to excitation, such as optical lattices. The idea is positioning atoms such that excitation to molecular resonances is not allowed. As shown in Appendix C, the loss can be suppressed by a factor of ~100, if the tightly trapped (~20 nm) individual atoms are prepared in a 3D optical lattice with the lattice constant tuned to avoid the resonances. By choosing the lattice constant, the outermost resonant shell  $R_\times = 6.2 \mu\text{m}$  can fall in a gap between density peaks, largely reducing its effect. High-fidelity manipulation of Rydberg atoms in a lattice has been observed recently [19]. Similar arguments apply to spatially separated optical traps: the distance between the traps should be larger than the radius of the outermost resonance shell.

To summarize, in this paper we investigated how molecular resonances limit the fidelity of Rydberg excitations in an atomic cloud. Under continuous driving pairs of atoms can be promoted into a doubly excited Rydberg states, if they are separated by certain resonant distances. These resonant pairs repel each other and leave the cloud. To mitigate this detrimental effect, trapping the atoms in a tight optical lattice can be used, where they are kept away from resonance.

## ACKNOWLEDGMENTS

We would like to thank E. Tiesinga and A. Kuzmich for discussions. This work was supported in part by the US National Science Foundation (NSF) Grant No. PHY-1212482. A.D. was also supported by the Simons Foundation as a

Simons fellow in theoretical physics. T.T. and A.D. would like to thank the Institute for Theoretical Atomic, Molecular and Optical Physics (ITAMP), Center for Ultracold Atoms, and the Harvard University Physics Department for their hospitality. Work at Harvard was supported by the NSF, CUA, AFOSR, MURI, and NSSEFF program.

#### APPENDIX A: DERIVATION OF THE MOLECULAR EXCITATION RATE IN THE IMPACT APPROXIMATION

As discussed in the main text, the collisions leading to strong coupling to molecular states are short and well separated. Let us consider one of such collisions of atom  $i$  with an atom  $j$ . The molecular probability amplitude satisfies the equation

$$i\dot{m}_{ij} = \Delta_{ij}m_{ij} + \frac{1}{2}\Omega_m^{ij}(c_i + c_j). \quad (\text{A1})$$

The detunings  $\Delta_{ij}$  [molecular potentials with the zero energy at the  $|r\rangle + |r\rangle$  dissociation limit,  $\Delta_{ij} = U(R_{ij}(t))$ ] and Rabi frequencies are time dependent because of the atomic motion. Introducing

$$m_{ij}(t) = \tilde{m}_{ij}(t) \exp\left[-i \int_{-\infty}^t \Delta_{ij}(t') dt'\right],$$

we recast Eq. (A1) into

$$i \frac{d}{dt} \tilde{m}_{ij}(t) = \frac{1}{2} \Omega_m^{ij} (c_i + c_j) \exp\left[i \int_{-\infty}^t \Delta_{ij}(t') dt'\right] \quad (\text{A2})$$

We are interested in the probability of molecular excitation due to a single collision,

$$P_m = |m_{ij}(\infty)|^2 = |\tilde{m}_{ij}(\infty)|^2.$$

Integrating Eq. (A2), we arrive at

$$\begin{aligned} \tilde{m}_{ij}(\infty) &= -i \int_{-\infty}^{\infty} \frac{1}{2} \Omega_m^{ij}(t) [c_i(t) + c_j(t)] \\ &\quad \times \exp\left\{i \int_{-\infty}^t U[R_{ij}(t')] dt'\right\} dt. \end{aligned} \quad (\text{A3})$$

To evaluate this probability we approximate  $R_{ij}(t)$  with straight-line trajectories,

$$R_{ij}(t) = \{[v(t - t_c)]^2 + \rho^2\}^{1/2}.$$

Here  $\rho$  is the conventional impact parameter,  $v$  is the relative atomic velocity, and  $t_c$  is the time of the closest approach. The atoms reach the resonance region when  $R_{ij}(t) = R_x$ . Clearly one has to require that  $\rho \leq R_x$  for this to occur. The associated moment of time  $t_x$  is

$$v(t_x^\pm - t_c) = \pm \sqrt{R_x^2 - \rho^2}.$$

The exponential in the integral (A3) rapidly oscillates except when the phase  $\int_{-\infty}^t U(R_{ij}(t')) dt'$  is stationary. The prefactor varies slowly in time compared to the exponent. This forms the basis for evaluating (A3) using the stationary-phase method. Let us review the basics of this method. Consider an integral

$$I = \int_{-\infty}^{+\infty} g(t) e^{i\phi(t)} dt,$$

where  $g(t)$  varies slowly compared to the rapidly oscillating exponent. The main value of the integral is accumulated in the regions where the phase is stationary, i.e.,

$$d\phi(t_*)/dt = 0.$$

Expanding the phase in the vicinity of the  $t_*$ :

$$\phi(t) \approx \phi(t_*) + \frac{1}{2} \phi''(t_*) (t - t_*)^2.$$

Then

$$\begin{aligned} I &\approx g(t_*) e^{i\phi(t_*)} \int_{-\infty}^{+\infty} \exp\left[i \frac{1}{2} \phi''(t_*) (t - t_*)^2\right] dt \\ &= g(t_*) e^{i\phi(t_*)} \exp\left\{i \frac{\pi}{4} \text{sgn}[\phi''(t_*)]\right\} \sqrt{\frac{2\pi}{|\phi''(t_*)|}}. \end{aligned}$$

In our case  $\phi(t) = \int_{-\infty}^t U(R_{ij}(t')) dt'$ , and the stationary points correspond to the crossing of the resonance shell

$$d\phi(t_*)/dt = U[R_{ij}(t_*)] = 0,$$

i.e.,  $t_* = t_x$ . Notice that we have two stationary points corresponding to two crossings of the resonance shell. The two times are separated by

$$t_x^+ - t_x^- = \frac{2\sqrt{R_x^2 - \rho^2}}{v}.$$

In general, both points can contribute. However, once promoted to the molecular state, the atoms experience strong mechanical forces and are accelerated out of the resonance. Therefore we will neglect the interference effects when computing the probability  $P_m$  and add the two contributions incoherently (this provides the upper limit on  $P_m$ ):

$$P_m = \pi \Omega_m^2 |c_i(t_x) + c_j(t_x)|^2 \left[ \frac{1}{|\phi''(t_x)|} \right].$$

Further we evaluate the second derivative of the phase evaluated at crossing points:

$$\begin{aligned} d^2\phi(t_x)/dt^2 &= \frac{dU}{dR_{ij}} \frac{dR_{ij}}{dt} = \frac{\Omega_m}{\Delta R_x} \frac{v}{R_x} v(t_x - t_c) \\ &= \frac{\Omega_m}{\Delta R_x} \frac{v}{R_x} \sqrt{R_x^2 - \rho^2}. \end{aligned}$$

From here one could define the effective duration of collision

$$\tau_c \approx \sqrt{\frac{\Delta R_x}{v} \frac{1}{\Omega_m}}$$

or

$$P_m = \pi |c_i(t_x) + c_j(t_x)|^2 \Omega_m \frac{\Delta R_x}{v} \frac{R_x}{\sqrt{R_x^2 - \rho^2}}.$$

We further approximate the time evolution of single Ry excitations via their uncoupled time evolution,  $c_k^I(t) = i/\sqrt{N} \sin[\sqrt{N}\Omega_0 t/2]$ :

$$P_m(\rho, t) = \frac{4\pi}{N} \Omega_m \frac{\Delta R_x}{v} \frac{R_x}{\sqrt{R_x^2 - \rho^2}} \sin^2[\sqrt{N}\Omega_0 t/2].$$

$P_m = 0$  for  $\rho > R_x$  as there are no crossing through the resonance region for such impact parameters.

The number of atoms lost due to a single collision is  $\Delta N = -2P_m$ . Now we sum the probabilities over multiple collisions. The number of atoms in a relative velocity group  $dv$  passing through the area  $2\pi\rho d\rho$  per time interval  $dt$  is equal to  $2\pi n\rho d\rho |v| f(v) d^3v dt$ , where  $n$  is the number density and  $f(v)$  is the velocity distribution. Then the compound atom loss satisfies the equation (here the factor of  $1/2$  is introduced to correct for double counting)

$$\frac{dN}{dt} = -2\gamma_m(t) \frac{N}{2} = -\gamma_m(t)N,$$

$$\gamma_m(t) = \iiint 2\pi n\rho d\rho |v| f(v) d^3v P_m.$$

Explicit evaluation yields the cross section

$$\begin{aligned} \sigma_m(t) &= 2\pi \int_0^{R_\times} \rho d\rho P_m(\rho, t) \\ &= (2\pi R_\times^2) \frac{4\pi}{N} \Omega_m \frac{\Delta R_\times}{v} \sin^2(\sqrt{N}\Omega_0 t/2) \end{aligned} \quad (\text{A4})$$

and the rate

$$\gamma_m(t) = n(2\pi R_\times^2) \frac{4\pi}{N} \Omega_m \Delta R_\times \sin^2(\sqrt{N}\Omega_0 t/2).$$

For a spherical volume of radius  $R_s$ ,  $n = 3N/(4\pi R_s^3)$ , thereby

$$\gamma_m(t) = 6\pi \left(\frac{R_\times}{R_s}\right)^3 \left(\frac{\Delta R_\times}{R_\times}\right) \Omega_m \sin^2(\sqrt{N}\Omega_0 t/2).$$

The rate equation has the solution

$$\begin{aligned} N(t) &= N(0) \exp\left[-\int_0^t \gamma_m(t') dt'\right], \\ \int_0^t \gamma_m(t') dt' &= \bar{\gamma}_m \left[ t - \frac{\sin(\sqrt{N}\Omega_0 t)}{2\sqrt{N}\Omega_0} \right], \\ \bar{\gamma}_m &= 3\pi \left(\frac{R_\times}{R_s}\right)^3 \left(\frac{\Delta R_\times}{R_\times}\right) \Omega_m. \end{aligned}$$

For sufficiently long time ( $t \gg 4\pi/(\sqrt{N}\Omega_0)$ ), the total number of atoms falls off exponentially as

$$N(t) = N(0) \exp(-\bar{\gamma}_m t).$$

Finally, the experiments are carried out with mesoscopic ensembles and as discussed in the main text, the radius of the resonance shell  $R_\times$  maybe comparable to  $R_s$  (or blockade radius). It is clear that if  $R_\times > 2R_s$ , the atoms are not going to be affected by that particular molecular resonance. We may further introduce a geometric probability factor  $g(R_\times/R_s)$

$$\gamma_m(t) \rightarrow \gamma_m(t) g(R_\times/R_s).$$

Further rates from multiple resonances add

$$\gamma_m(t) \rightarrow \sum_k \gamma_m^k(t),$$

where  $\gamma_m^k$  is the rate due to an individual resonance shell at  $R_\times^k$ .

## APPENDIX B: DERIVATION OF THE INHOMOGENEOUS BROADENING

In the main body it is mentioned that the molecular resonances have more consequences than just leading to the molecular rate  $\gamma_m$ . Here we consider the additional loss of coherence by inhomogeneous broadening.

### 1. Hamiltonian

We assume that the  $N$  identical atoms move negligibly over the entire extent of the dynamics in question, so we need to track only the electronic degrees of freedom. We model each atom as a four-level system, with states  $|g\rangle, |r\rangle, |r'\rangle, |r''\rangle$ . Let us define the following collective states,

$$|G\rangle = |g\rangle^{\otimes N}, \quad (\text{B1})$$

$$|j\rangle = \sigma_j^\dagger |G\rangle, \quad (\text{B2})$$

$$|j, k\rangle = \sigma_j^\dagger \sigma_k^\dagger |G\rangle, \quad (\text{B3})$$

where  $\sigma_j = |g\rangle_j \langle r|_j$ ,  $\sigma_j' = |g\rangle_j \langle r'|_j$ , and  $\sigma_j'' = |g\rangle_j \langle r''|_j$ , ( $j \neq k$ ). An external driving field coherently couples  $|g\rangle$  with  $|r\rangle, |r'\rangle$ , and  $|r''\rangle$ . When two atoms are in  $|r'r''\rangle$  or  $|r''r'\rangle$  states, they interact via the Rydberg interaction. The resulting Hamiltonian is

$$\begin{aligned} H &= \sum_j \frac{\Omega_0}{2} (|G\rangle \langle j| + \text{H.c.}) \\ &+ \sum_{j,k} \frac{\Omega_m}{2} (|j\rangle \langle j, k| + |j\rangle \langle k, j| + \text{H.c.}) \\ &+ \sum_{j,k} \Delta_{jk} |j, k\rangle \langle j, k|. \end{aligned} \quad (\text{B4})$$

In the ideal case, when  $\Delta_{jk} \rightarrow \infty$ ,  $|G\rangle$  is coherently coupled to the symmetric combination of a single excitation,

$$|S\rangle = \frac{1}{\sqrt{N}} \sum_j |j\rangle, \quad (\text{B5})$$

and the resulting dynamics is a Rabi oscillation between  $|G\rangle$  and  $|S\rangle$ , with Rabi frequency  $\Omega_R = \sqrt{N}\Omega_0$ , if the system starts in  $|G\rangle$ .

To investigate the deviation of the real dynamics from the ideal one, we focus on the coupling of  $|j, k\rangle$  states to  $|S\rangle$ . Using this notation the Hamiltonian can be written as

$$\begin{aligned} H &= \frac{\sqrt{N}\Omega_0}{2} (|G\rangle \langle S| + \text{H.c.}) \\ &+ \sum_{j,k>j} \frac{\Omega_m}{\sqrt{N}} (|S\rangle \langle M_{jk}| + \text{H.c.}) \\ &+ \sum_{j,k>j} \Delta_{jk} |M_{jk}\rangle \langle M_{jk}|, \end{aligned} \quad (\text{B6})$$

where  $|M_{jk}\rangle = \frac{|j,k\rangle + |k,j\rangle}{\sqrt{2}}$ , and the nonsymmetric combinations are not coupled to  $|S\rangle$ .

## 2. Broadening

We adiabatically eliminate the doubly excited states  $\{|j, k\rangle\}$  from Eq. (B6) to arrive at the effective Hamiltonian,

$$H_{\text{eff}} = h_{\Omega_0} + \sum_j \left( \Delta_j - i \frac{\Gamma_j}{2} \right) |j\rangle \langle j| + \sum_{j, k > j} \frac{\Omega_{jk}}{2} (|j\rangle \langle k| + |k\rangle \langle j|), \quad (\text{B7})$$

where  $h_{\Omega_0}$  is the first term in Eq. (B6), and the new coefficients are

$$\Delta_j = - \sum_{k \neq j} \frac{\Omega_m^2}{4} \frac{\mathcal{P}}{\Delta_{jk}}, \quad (\text{B8})$$

$$\Omega_{jk} = - \frac{\Omega_m^2}{2\Delta_{jk}}, \quad (\text{B9})$$

$$\Gamma_j = 2\pi \sum_{k \neq j} \Omega_m^2 \delta(\Delta_{jk}), \quad (\text{B10})$$

where  $\mathcal{P}$  indicates principal value. The  $\Gamma_j$  terms describe the resonant excitation, which is as discussed in the previous section and lead to the molecular decay rate  $\gamma_m$ .

The  $j$  dependence of  $\Delta_j$  results in inhomogeneous broadening,  $\delta\Delta := \sqrt{\langle \Delta^2 \rangle - \langle \Delta \rangle^2}$ .

$$\begin{aligned} \delta\Delta &= \frac{\Omega_m^2}{4} \sqrt{\text{Var} \left( \sum_{k \neq j} - \frac{\mathcal{P}}{\Delta_{jk}} \right)} \\ &= \frac{\Omega_m^2}{4} \sqrt{\text{Var} \left( \sum_{k \neq j} \frac{\mathcal{P}}{\Delta_E} \frac{R_{jk}^3}{R_{jk}^3 - R_\times^3} \right)}, \end{aligned} \quad (\text{B11})$$

where we used  $\Delta_{jk} = U(R_{jk}) = \frac{C_3}{R_{jk}^3} - \Delta_E$ , i.e., a van der Waals interaction potential between the Rydberg atoms and eliminated  $C_3$  by using that  $R_\times^3 = \frac{C_3}{\Delta_E}$ .

The sum can be written as

$$\begin{aligned} D_j &:= \sum_{k \neq j} \frac{\mathcal{P}}{\Delta_E} \frac{R_{jk}^3}{R_{jk}^3 - R_\times^3} \\ &= \frac{N}{V\Delta_E} \int_V d^3\mathbf{r}_k \frac{\mathcal{P} |\mathbf{r}_k - \mathbf{r}_j|^3}{|\mathbf{r}_k - \mathbf{r}_j|^3 - R_\times^3} \\ &= \frac{N}{V\Delta_E} \int_{V'} d^3\mathbf{r} \frac{\mathcal{P} r^3}{r^3 - R_\times^3}, \end{aligned} \quad (\text{B12})$$

where the integrand is more conveniently written in terms of  $r = |\mathbf{r}| = |\mathbf{r}_k - \mathbf{r}_j|$ .  $\mathbf{r}$  can be seen as “local” spherical coordinate, centered around  $\mathbf{r}_j$ . Due to global rotational invariance of the problem we can set  $\mathbf{r}_j = r_j \hat{\mathbf{z}}$  without loss of generality. We then find (see Sec. B4)

$$\begin{aligned} \frac{D_j V \Delta_E}{N} &= \int_0^{R-r_j} 4\pi r^2 \frac{\mathcal{P} r^3}{r^3 - R_\times^3} dr \\ &+ \int_{R-r_j}^{R+r_j} 2\pi r^2 \frac{\mathcal{P} r^3}{r^3 - R_\times^3} \left( 1 - \frac{r^2 + r_j^2 - R^2}{2rr_j} \right) dr. \end{aligned} \quad (\text{B13})$$

We now assume that the singularity is in the first integral,  $R_\times < R - r_j$ . As a result, the second integral is no longer a principal value integral and since  $r \geq R - r_j > R_\times$  we will furthermore approximate  $\frac{r^3}{r^3 - R_\times^3} \approx 1$ . The second integral is then straightforward to evaluate. Finally we use the indefinite integral

$$\int \frac{r^5}{r^3 - R_\times^3} dr = \frac{1}{3} r^3 + \frac{1}{3} R_\times^3 \ln(r^3 - R_\times^3) \quad (\text{B14})$$

to find the remaining principal value integral. The result is

$$D_j = \frac{N}{\Delta_E} \left\{ 1 + \left( \frac{R_\times}{R} \right)^3 \ln \left[ \left( \frac{R - r_j}{R_\times} \right)^3 - 1 \right] \right\}. \quad (\text{B15})$$

Now we can determine the averages  $\langle D \rangle$  and  $\langle D^2 \rangle$ , but since the above expression for  $D_j$  is valid only when  $r_j < R - R_\times$  we modify the averages to only average over a sphere with radius  $R - R_\times$ :

$$\begin{aligned} \langle D \rangle &= \frac{1}{N} \sum_j D_j = \frac{1}{V} \int_V d^3\mathbf{r}_j D_j \\ &\approx \frac{3}{2(R - R_\times)^3} \int_0^{R-R_\times} r_j^2 D_j dr_j, \end{aligned} \quad (\text{B16})$$

$$\begin{aligned} \langle D^2 \rangle &= \frac{1}{N} \sum_j (D_j)^2 = \frac{1}{V} \int_V d^3\mathbf{r}_j (D_j)^2 \\ &\approx \frac{3}{2(R - R_\times)^3} \int_0^{R-R_\times} r_j^2 (D_j)^2 dr_j, \end{aligned} \quad (\text{B17})$$

where we also used that  $D_j$  only depends on  $r_j = |\mathbf{r}_j|$ . Since we are interested in the regime where  $R_\times \ll R$ , these approximations actually do not differ much from the true averages. Then using the expansion

$$D_j = \frac{N}{\Delta_E} \left[ 1 - 3 \left( \frac{R_\times}{R} \right)^3 \ln \left( \frac{R_\times}{R - r_j} \right) + \dots \right], \quad (\text{B18})$$

the averages can be found by a direct evaluation of the integrals above. The resulting expression for the variance in  $D_j$  is then found to be, up to lowest order in  $\frac{R_\times}{R}$ :

$$\delta D = \sqrt{\langle D^2 \rangle - \langle D \rangle^2} = \frac{7}{2} \frac{N}{\Delta_E} \left( \frac{R_\times}{R} \right)^3. \quad (\text{B19})$$

With this result we can write the broadening  $\delta\Delta$  as

$$\delta\Delta = \frac{\Omega_m^2}{4} \delta D = \frac{7}{2} \pi \rho_d \Omega_m^2 \frac{R_\times^2}{|U'(R_\times)|}, \quad (\text{B20})$$

where the quadratic dependency on  $R_\times$  was also reproduced using numerical calculations and in fact is the same as for the molecular rate  $\gamma_m$ . This whole calculation can be directly reused for another potential, van der Waals, for example,  $U(R_{jk}) = \frac{C_6}{R_{jk}^6} - \Delta_E$ . The result is

$$\delta\Delta = \sqrt{\frac{12}{5}} \pi \rho_d \Omega_m^2 \frac{R^2}{|U'(R_\times)|} \left( \frac{R_\times}{R} \right)^{5/2}, \quad (\text{B21})$$

where again the power of  $R_\times$  is consistent with numerics.

### 3. Effect on coherence

The effect of this inhomogeneous broadening is well approximated by an additional decay of the coherence between the ground state  $|G\rangle$  and the symmetric single-excitation state  $|S\rangle = \sum_i |R_i\rangle/N$ , by a factor of  $e^{-(\delta\Delta)^2}$ . This is a much weaker effect than the pure exponential decay, set by  $\gamma_m$ , and since  $\delta\Delta \lesssim \gamma_m$  for the parameter regime in consideration, the effect of inhomogeneous broadening can be neglected as long as  $\gamma_m t < 1$ .

### 4. Local spherical coordinates

For completeness we briefly describe the “local” spherical coordinates mentioned in the above derivation. In favor of symmetry of the integrand we make the substitution  $\mathbf{r} = \mathbf{r}_k - \mathbf{r}_j$ , which requires changing the boundaries of the polar integral. Without loss of generality we can take  $\mathbf{r}_j$  on the  $z$  axis. Then, depending on the relation between  $r, r_j$ , and  $R$  there are three regions. First, if  $r < R - r_j$ , then the entire sphere of radius  $r = |\mathbf{r}|$  lies within the boundaries of the cloud, and therefore we have  $0 \leq \theta \leq \pi$ . Similarly, if  $r > R + r_j$ , then the opposite is true: the cloud lies entirely inside the sphere of radius  $r$ , and therefore there is no contribution to the integral from this part.

If  $R - r_j < r < R + r_j$ , then there exists a circle, where the sphere of radius  $r$  intersects the boundary of the cloud, as shown in Fig. 3. The angle between the segments  $r_j$  and  $r$  is

$$\pi - \theta_c = \arccos\left(\frac{r^2 + r_j^2 - R^2}{2rr_j}\right), \quad (\text{B22})$$

and therefore we have  $\theta_c \leq \theta \leq \pi$ . Defining  $\theta_0$  as the lower bound of the  $\theta$  integral, we have  $\theta_0(r < R - r_j) = 0$  and  $\theta_0(R - r_j < r < R + r_j) = \theta_c$ , so that we can rewrite the

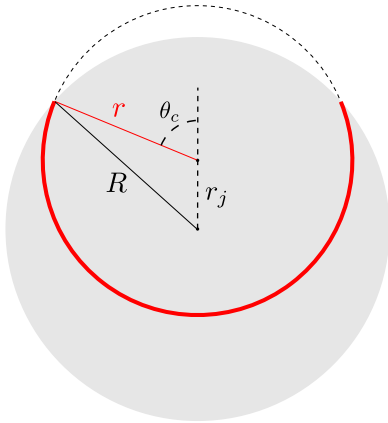


FIG. 3. (Color online) We only need to integrate over that part (red) of the dotted sphere that is inside the cloud. This corresponds to a modification of the boundaries for the  $\theta$  integral, depending on the relation between  $r, r_j$ , and  $R$ . The figure shows the case when  $R - r_j < r < R + r_j$ .

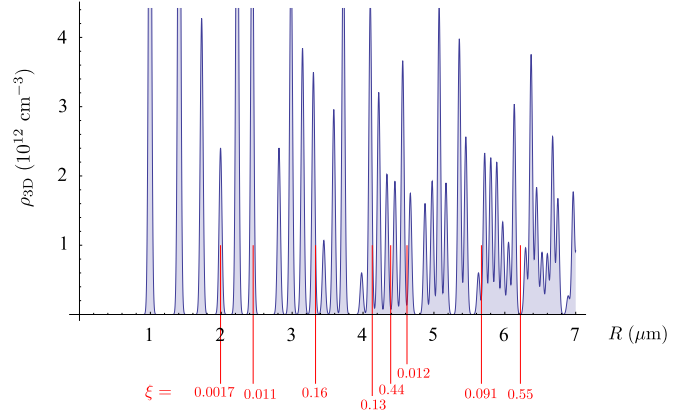


FIG. 4. (Color online) 3D density of the atoms in a cubic lattice (lattice constant:  $a = 0.995 \mu\text{m}$ ) as a function of distance,  $R$ . Each atom is confined by a harmonic trap to a region of size  $d = 0.02 \mu\text{m}$ . Red vertical lines indicate the position of the resonances given in Table I. The numbers shown next under the lines are the molecular coupling coefficients,  $\xi_i$ , for each resonance.

integral in Eq. (B12) as

$$\begin{aligned} \int_{V'} d^3\mathbf{r} f(r) &= \int_0^{R+r_j} r^2 dr \int_{\theta_0(r)}^{\pi} \sin(\theta) d\theta \int_0^{2\pi} d\phi f(r) \\ &= \int_0^{R-r_j} 4\pi r^2 f(r) dr \\ &\quad + \int_{R-r_j}^{R+r_j} 2\pi r^2 f(r) \left(1 - \frac{r^2 + r_j^2 - R^2}{2rr_j}\right) dr, \end{aligned} \quad (\text{B23})$$

where  $f(r)$  is the integrand that only depends on  $r$ .

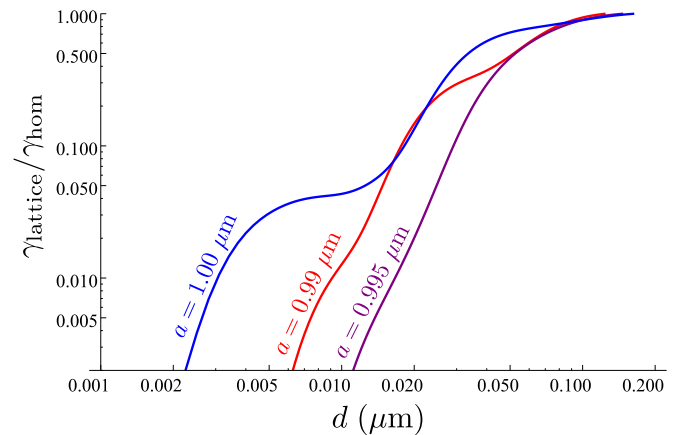


FIG. 5. (Color online) Decay rate in a 3D lattice normalized with the homogeneous decay rate result for lattice constants  $a = 1.00, 0.99$ , and  $0.995 \mu\text{m}$ . The suppression is strong for small trap size, and diminishes ( $\gamma_{\text{lattice}} \rightarrow \gamma_{\text{hom}}$ ) for large size. Small changes in  $a$  result in significant changes in the suppression. This is due to the detailed peak structure of the 3D density in the lattice. As a result, fine tuning of the lattice constant is required.

### APPENDIX C: SUPPRESSION OF RESONANCE BY TRAPPING IN REGULAR LATTICE

We investigate the possibility of trapping the atoms in an 3D cubic optical lattice, in order to suppress the effective decay rate  $\gamma$ , due to double Rydberg resonances. We use the homogeneous atom density case as a benchmark,

$$\gamma_{\text{hom}} = \sum_j \gamma_j = 2\pi^2 \Omega_0 \rho \sum_i \xi_i R_{\times,i}^2 \Delta R_{\times,i}, \quad (\text{C1})$$

where the summation is performed over all resonances at the crossing distances  $R_{\times,i}$ , each having a width of  $\Delta R_{\times,i}$  and molecular coupling factor  $\xi_i$ . Here  $\rho$  is assumed to be constant.

We assume that in a 3D cubic lattice, each lattice site holds a single atom, trapped in the ground state of the harmonic trap. Let  $a$  denote the lattice constant and  $d$  be the size of each

trapped wave function. The deeper we make the lattice, the smaller the  $d/a$  ratio can be. For given  $d, a$  values, we can plot the 3D density  $\rho(R)$  of the atoms as a function of distance from a particular lattice site. This is shown in Fig. 4 with a blue curve.

By taking the  $R$  dependence of the atom density  $\rho(R)$  into account, we can write the total decay rate as

$$\gamma_{\text{lattice}} = \sum_j \gamma_j = 2\pi^2 \Omega_0 \sum_i \rho(R_{\times,i}) \xi_i R_{\times,i}^2 \Delta R_{\times,i}, \quad (\text{C2})$$

numerically evaluate, and compare it with the homogeneous result,  $\gamma_{\text{hom}}$ . In Fig. 5 we plot  $\gamma_{\text{lattice}}/\gamma_{\text{hom}}$  as a function of the trap confinement  $d$  for different fixed values of  $a$ . A confinement of  $d/a \approx 0.01$  can suppress the decay to 2%–10% of its homogeneous density value, depending on the accuracy of the fine tuning of the lattice constant.

- 
- [1] M. D. Lukin, M. Fleischhauer, R. Cote, L. M. Duan, D. Jaksch, J. I. Cirac, and P. Zoller, *Phys. Rev. Lett.* **87**, 037901 (2001).
- [2] D. Jaksch, J. I. Cirac, P. Zoller, S. L. Rolston, R. Cote, and M. D. Lukin, *Phys. Rev. Lett.* **85**, 2208 (2000).
- [3] M. D. Lukin, *Rev. Mod. Phys.* **75**, 457 (2003).
- [4] M. Saffman, T. G. Walker, and K. Molmer, *Rev. Mod. Phys.* **82**, 2313 (2010).
- [5] L. Isenhower, E. Urban, X. L. Zhang, A. T. Gill, T. Henage, T. A. Johnson, T. G. Walker, and M. Saffman, *Phys. Rev. Lett.* **104**, 010503 (2010).
- [6] A. Gaëtan, Y. Miroshnychenko, T. Wilk, A. Chotia, M. Viteau, D. Comparat, P. Pillet, A. Browaeys, and P. Grangier, *Nat. Phys.* **5**, 115 (2009).
- [7] H. Kübler, J. P. Shaffer, T. Baluksian, R. Löw, and T. Pfau, *Nat. Photon.* **4**, 112 (2010).
- [8] C. S. Hofmann, G. Günter, H. Schempp, M. Robert-De-Saint-Vincent, M. Gärtner, J. Evers, S. Whitlock, and M. Weidemüller, *Phys. Rev. Lett.* **110**, 203601 (2013).
- [9] O. Firstenberg, T. Peyronel, Q.-Y. Liang, A. V. Gorshkov, M. D. Lukin, and V. Vuletic, *Nature (London)* **502**, 71 (2013).
- [10] Y. O. Dudin, L. Li, F. Bariani, and A. Kuzmich, *Nat. Phys.* **8**, 790 (2012).
- [11] M. Ebert, M. Kwon, T. G. Walker, and M. Saffman, *Phys. Rev. Lett.* **115**, 093601 (2015).
- [12] T. Keating, K. Goyal, Y. Y. Jau, G. W. Biedermann, A. J. Landahl, and I. H. Deutsch, *Phys. Rev. A* **87**, 052314 (2013).
- [13] Y. V. Dumin, *J. Phys. B* **47**, 175502 (2013).
- [14] Y. Hahn, *J. Phys. B* **33**, L655 (2000).
- [15] K. Blum, *Density Matrix Theory and Applications*. Springer Series on Atomic, Optical, and Plasma Physics (Springer, Berlin, 2012).
- [16] H. Georgi, *The Physics of Waves* (Benjamin Cummings, Englewood Cliffs, NJ, 1992).
- [17] E. Urban, T. A. Johnson, T. Henage, L. Isenhower, D. D. Yavuz, T. G. Walker, and M. Saffman, *Nature Phys. (London)* **5**, 110 (2009).
- [18] T. A. Johnson, E. Urban, T. Henage, L. Isenhower, D. D. Yavuz, T. Walker, and M. Saffman, *Phys. Rev. Lett.* **100**, 113003 (2008).
- [19] J. Zeiher, P. Schauß, S. Hild, T. Macrì, I. Bloch, and C. Gross, *Phys. Rev. X* **5**, 031015 (2015).